Kidney International, Vol. 64 (2003), pp. 1580–1587

Mutations of the *Uromodulin* gene in MCKD type 2 patients cluster in exon 4, which encodes three EGF-like domains

Matthias T.F. Wolf, Bettina E. Mucha, Massimo Attanasio, Isabella Zalewski, Stephanie M. Karle, Hartmut P.H. Neumann, Nazneen Rahman, Birgit Bader, Conrad A. Baldamus, Edgar Otto, Ralph Witzgall, Arno Fuchshuber, and Friedhelm Hildebrandt

Department of Pediatrics and Communicable Diseases, University of Michigan, Ann Arbor, Michigan; University Children's Hospital, Freiburg University, Freiburg, Germany; Department of Internal Medicine, University Hospital, Freiburg University, Freiburg, Germany; Section of Cancer Genetics, Institute of Cancer Research, Sutton, United Kingdom; Department of Internal Medicine, University Hospital, Tuebingen University, Tuebingen, Germany; Department of Internal Medicine, University Hospital, Cologne University, Cologne, Germany; and Institute for Molecular and Cellular Anatomy, University of Regensburg, Regensburg, Germany

Mutations of the *Uromodulin* gene in MCKD type 2 patients cluster in exon 4, which encodes three EGF-like domains.

Background. Autosomal-dominant medullary cystic kidney disease type 2 (MCKD2) is a tubulointerstitial nephropathy that causes renal salt wasting, hyperuricemia, gout, and end-stage renal failure in the fifth decade of life. The chromosomal locus for MCKD2 was localized on chromosome 16p12. Within this chromosomal region, Uromodulin *(UMOD)* was located as a candidate gene. *UMOD* encodes the Tamm-Horsfall protein. By sequence analysis, one group formerly excluded *UMOD* as the disease-causing gene. In contrast, recently, another group described mutations in the *UMOD* gene as responsible for MCKD2 and familial juvenile hyperuricemic nephropathy (FJHN).

Methods. Haplotype analaysis for linkage to *MCKD2* was performed in 25 MCKD families. In the kindreds showing linkage to the *MCKD2* locus on chromosome 16p12, mutational analysis of the *UMOD* gene was performed by exon polymerase chain reaction (PCR) and direct sequencing.

Results. In 19 families, haplotype analysis was compatible with linkage to the *MCKD2* locus. All these kindreds were examined for mutations in the *UMOD* gene. In three different families, three novel heterozygous mutations in the *UMOD* gene were found and segregated with the phenotype in affected individuals. Mutations were found only in exon 4.

Conclusion. We confirm the *UMOD* gene as the disease-causing gene for MCKD2. All three novel mutations were found in the fourth exon of *UMOD*, in which all mutations except one (this is located in the neighboring exon 5) published so far are located. These data point to a specific role of exon 4 encoded sequence of *UMOD* in the generation of the MCKD2 renal phenotype.

Key words: MCKD2, uromodulin, Tamm-Horsfall protein.

Received for publication March 20, 2003
and in revised form May 28, 2003
Accepted for publication June 23, 2003

Medullary cystic kidney disease type 2 (MCKD2) (OMIM 603860) includes clinical features of reduced urinary concentration, salt wasting, and end-stage renal failure. In contrast to MCKD1, in MCKD2, a more severe phenotype concerning hyperuricemia and gout has been described. Moreover, in MCKD2, an earlier median age of onset has been reported (age of onset in MCKD2 is 32 years of age compared to 62 years in MCKD1) [1]. Otherwise, these two diseases are clinically undistinguishable. In MCKD, small corticomedullary cysts are common, but not always detected. Kidney size is normal or slightly reduced. MCKD shows a renal histologic triad of (*1*) tubular basement disintegration, (*2*) tubular atrophy with cyst development at the corticomedullary border, and (*3*) interstitial cell infiltration associated with fibrosis [2]. Neither imaging results, nor pathologic findings, are pathognomic for MCKD2. The condition shares clinical and morphologic similarities to recessive juvenile nephronophthisis (NPH) [3]. In contrast to juvenile onset in NPH, end-stage renal failure in MCKD occurs in adulthood. Moreover NPH is inherited in an autosomal-recessive pattern, whereas MCKD is autosomal-dominant.

Two loci for MCKD have been described: *MCKD1* showed linkage to chromosome 1q21 in two Cypriot families [4] and *MCKD2* was localized on chromosome 16p12 in an Italian family [1]. Two groups showed independently that loci for familial juvenile hyperuremic nephropathy (FJHN) and MCKD2 mapped to the same chromosomal region on 16p12 [5, 6], assuming that FJHN and MCKD2 might be different facets of the same disease caused by mutations in one and the same gene. Later, an additional FJHN locus was mapped to a more centromeric region [7] on chromosome 16, resulting in

two different FJHN loci, which are overlapped by the *MCKD2* locus [8]. Two years after publication of the chromosomal candidate region of *MCKD2*, Uromodulin (*UMOD*) was published as excluded from representing the disease-causing gene [9]. In contrast however, Hart et al [10] later detected four different mutations in the *UMOD* gene, indicating that this is the gene responsible for FJHN and MCKD2.

UMOD encodes the Tamm-Horsfall protein (THP), which is expressed primarily at the luminal side of renal epithelial cells of the thick ascending loop of Henle and of early distal convoluted tubules. THP is the most abundant protein in the urine of humans [11]. Functional roles of *UMOD* have been described in urinary tract infections, in binding to complement factors, in myeloma kidney, and nephrolithiasis [12–15]. The *UMOD* protein contains (*1*) a zona pellucida domain (ZP), which is necessary for polymerization into the supramolecular structure of a filament, (*2*) an elastase-sensitive fragment containing three calcium-binding epidermal growth factor (EGF)-like domains and a signal peptide, and (*3*) a potential glycosyl-phosphatidylinositol (GPI)-anchor cleavage site. *UMOD* is a transmembrane-bound protein, which can be secreted into the urine by cleavage of the GPI-anchor [16].

We here report three novel mutations in *UMOD* and confirm *UMOD* as the disease-causing gene. So far, eight mutations published are located in exon 4 and one mutation was found at the beginning of the neighboring exon 5 of the *UMOD* gene that encodes three EGF-like domains [10, 17].

METHODS

Patients

We ascertained 25 MCKD families (224 individuals, of which 84 were affected). Fourteen families were from Germany, three from the United States, two each from the United Kingdom, Hungary, and Turkey, respectively, one each from Belgium and China, respectively. The age at diagnosis, the age at onset of end-stage renal disease (ESRD), hyperuricemia, imaging data, and biopsy results were reviewed if available. Clinical criteria necessary for inclusion were (*1*) compatibility of pedigree with autosomal-dominant inheritance, (*2*) chronic renal failure, (*3*) defective urine concentration (<800 mOsm/L after overnight dehydration) with polyuria (>3 L/day), and (*4*) at least one pedigree member with chronic renal failure in whom renal biopsy showed tubulointerstitial fibrosis with infiltrates, tubular atrophy, and thickening of the tubular basement membrane. Optional clinical criteria were normal or small-sized kidneys with occasional small corticomedullary cysts. Hyperuricemia was defined as serum uric acid concentration >1 SD greater than the normal values for age and gender (both genders 5 to 10 years, 4.1 ± 1 mg/dL; female, 12 years, 4.5 ± 0.9 mg/dL; 15 years, 4.5 ± 0.9 mg/dL; ≥18 years, 4.0 ± 0.7 mg/dL; male, 12 years, 4.4 ± 1.1 mg/dL; 15 years, 5.5 ± 1.1 mg/dL; ≥18 years, 6.2 ± 0.8) [18].

The study was approved by the Ethics Committee of the Albert-Ludwigs-University Freiburg and all participating family members provided informed consent.

Haplotype analysis

Genomic DNA was isolated by standard methods directly from blood samples using the QIAamp blood kit (Qiagen, Valencia, CA, USA) or from blood lymphocytes after Epstein-Barr virus (EBV) transformation. Haplotype analysis was performed in 224 individuals (including 84 affected individuals) and inferred in 18 additional individuals (nine additional affected individuals), using 13 consecutive polymorphic microsatellite markers that span the critical *MCKD2* region in the following order: cen-D16S3116-D16S401-D16S3113-D16S420-D16S417-D16S412-D16-S3036-D16S3041-D16S3056-D16S501-D16S499-D16S-3060-D16S764-tel. Fluorescently labeled polymerase chain reaction (PCR) products were detected by a Genetic Analyzer 3100 (Applied Biosystems, Foster City, CA, USA) and were analyzed by the GENOTYPER software.

Mutational analysis of the *UMOD* gene

Mutational analysis was performed by exon PCR of the *Uromodulin* gene. Primer sequences were determined using the UCSC sequence (November 2002 freeze) encompassing the coding sequence of *UMOD* [19]. The following primers and conditions were employed: exon 3, 5′-CAATCAAAGCACTCCTTCCAG-3′ and 5′-GACAGGTGCTACATTGCTTCC-3′; exon 4 was divided into two different overlapping parts: exon 4a, 5′-CCTGGAGAATGAGGGAAGG-3′ and 5′-CTG GACGAGTACTGGCGC-3′; exon 4b, 5′-GGCAGCT ACTTGTGCGTATG-3′ and 5′-CTCTGCAGTGCCT TTCCAG-3′; exon 5, 5′-GTCTCCCCACAGTCCTC ATC-3′ and 5′-GGCAGTGACAGGTTTCTCAAC-3′; exon 6, 5′-GGCCCCCAAGCTATAGACAC-3′ and 5′-CCATGAATTGCTTTCTTTATTTG-3′; exon 7,5′-TCATGCCCCTTTCTCTCATC-3′ and 5′-GCTCATG GTTAAGGGGTTTG-3′; exon 8, 5′-TGCCTAGGA ATGCAAATCAG-3′ and 5′-CCTTACCTGTCCTGG ATGATG-3′; exon 9, 5′-TCAGCTCTGCACTGATGA CAG-3′ and 5′-TGGCCAAATGTCTTTGGTTAC-3′; exon 10, 5′-AACCACATTCAGGCTCCTTC-3′ and 5′-AGGTGCCAGGCTCTGTTATC-3′; exon 11, 5′-GTCAGGATGCTTGCCAAATC-3′ and 5′-CACTG CAGAAAGGACCTGAAC-3′; and exon 12, 5′-GG GTGTCCTCTTCTGATTGG-3′ and 5′-CAGGTA CACCGTCACAAGTCC-3′ using a "touch down" program with a starting annealing temperature of 72°C (exons 4a, 5, and 10), decreasing every step by 0.7°C for 24

times and a next round of amplification with an annealing temperature of 55°C for 20 times. An annealing temperature of 60°C was used for the exons 3, 4b, 8, and 9, 59°C for exons 7, 11, and 12, and 57°C for exon 6. PCR products were purified using the Marligen Rapid PCR Purification System (Ijamsville, MD, USA). Purified PCR products were sequenced, using a Genetic Analyzer 3700 (Applied Biosystems) and resulting sequences were evaluated with the Sequencher Software (Gene Codes, Ann Arbor, MI, USA).

RESULTS

Clinical data

The three families presenting with *UMOD* mutations included 12 living individuals affected with MCKD (three in F524, three in F739 and six in F762) (Fig. 1). Six of 12 also suffered from hyperuricemia (Table 1). The patients presented with hyperuricemia between 17 and 59 years of age (Table 1). ESRD developed between 29 years and 60 years. Imaging by magnetic resonance imaging (MRI) or ultrasound revealed in all families suspicious results with small kidneys, decreased parenchyma, or cysts. Occasional small cysts were only visible in three individuals by ultrasound (Table 1). Renal histology in all cases was compatible with MCKD showing microcysts in four out of 12 cases and in the others dilated or atrophied tubules, global sclerosis, extensive tubulointerstitial atrophy with fibrosis, and signs of chronic diffuse inflammation (Table 1).

Linkage analysis

In 25 families with 224 individuals, haplotype analysis for linkage to *MCKD1* and *MCKD2* was performed. In one kindred (F762), we found significant linkage to *MCKD2.* In six kindreds, significant linkage to chromosome 1 [logarithm of odds (LOD) score >3.0] or exclusion of linkage to chromosme 16 was found. Linkage for family F762 was previously published with a maxiumum multipoint LOD score of 3.75 in the interval between D16S3017 and D16S417 [20]. In 19 families too small for significant linkage, haplotype analysis was compatible with linkage to MCKD2.

Mutation analysis

We performed mutational analysis in affected individuals from 19 families compatible with linkage to *MCKD2* examining all 10 coding exons of the *UMOD* gene by exon PCR and direct sequencing of the forward strands of exon PCR products.

We used an "affecteds only" approach for definition of the affected status of MCKD. Specifically, if diagnostic data supported MCKD, the affected status was assumed. If there was no data demonstrating the presence of MCKD, the disease status was determined as unknown, since there is age-related penetrance in MCKD. On this basis, there was full-cosegregation of all found heterozygous *UMOD* mutations and the affected status for MCKD.

In three of these families, novel mutations were detected (Fig. 1). All three mutations were located in exon 4. In family F524, a nucleotide exchange (C779A) was found, resulting in the amino acid exchange Thr225Lys. The mutation was identified in all three affected brothers. Because I-1 in F524 is deceased, we cannot prove that he had the same mutation. His treatment of 15 years of dialysis makes his affected status very likely.

In family F739, a C849G mutation was detected, causing the amino acid exchange Cys248Trp. The mutation in F762 is an inframe deletion/insertion at position 383 (383del12/ins9) that deletes five amino acids and inserts four new amino acids.

Moreover, none of the mutations were found in 100 healthy controls. Therefore, our detected mutations are unlikely to be common polymorphisms.

In exon 6, an additional substitution (G1477T, Val458Leu) was found in two families that were compatible with linkage to 16p12. Nevertheless, this substitution was realized to be a new single nucleotide polymorphism (SNP) because we detected it in four healthy controls out of 100.

DISCUSSION

We detected three novel heterozygous mutations in the *UMOD* gene, thereby confirming that *UMOD* is the responsible gene for MCKD2. All detected mutations are found in exon 4 of *UMOD,* thus underlining the specific role of exon 4–encoded sequence in the generation of the MCKD2 renal phenotype.

In previous studies, abnormal localization of *UMOD* protein in the interstitium in MCKD patients was shown, suggesting *UMOD* as a candidate gene for MCKD [21]. By identifying three novel mutations, we confirmed the *UMOD* gene as the responsible gene for MCKD2. All mutations described here affect amino acids conserved in the cow, mouse, and rat (Fig. 2). The mutation of F762 (383del12/ins9) is positioned in a domain of known function, the second calcium binding (cb) EGF-like domain. In F762, the cbEGF-like domain encoded by *UMOD* exon 4 is affected by a loss of five amino acids and their replacement by four new amino acids. Two of the five amino acids involved by the mutation of F762 are highly conserved in evolution, including the lower vertebrate zebrafish and the nematode *Caenorhabditis elegans,* in genes encoding EGF binding domains (for example, fibulin 1, an EGF containing extracellular matrix protein). In a number of human diseases, including Marfan syndrome, cerebral autodomal-dominant arteriopathy with subcortical infarcts and leukencephalopathy (CADASIL), Alagille syndrome, protein S defi-

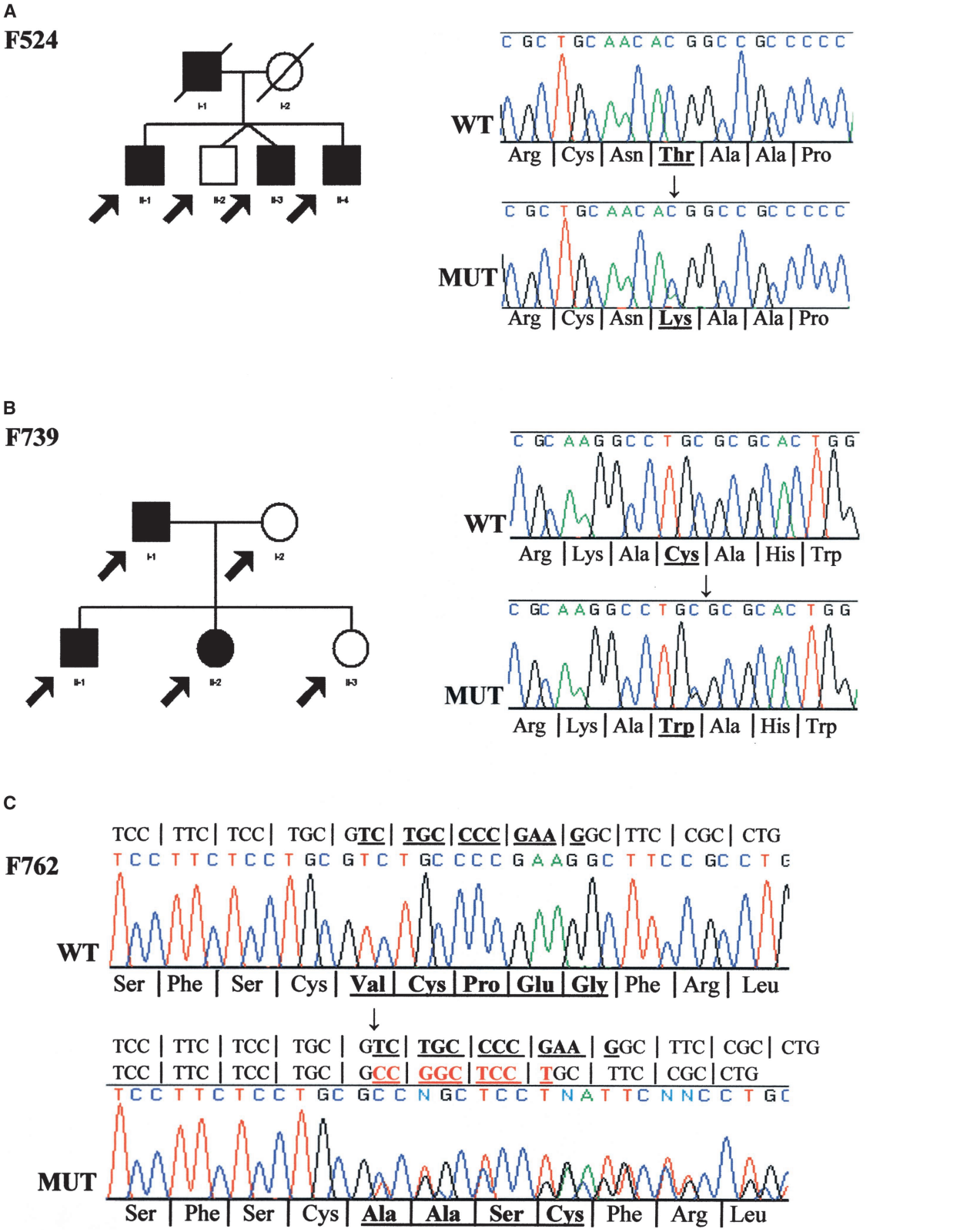

Fig. 1. Mutations in the *Uromodulin* (*UMOD*) gene. The upper sequence shows the wild-type (WT) sequence and the lower sequence reveals the mutation (MUT) in each family. The resulting amino acids are indicated below sequences. All mutations are located in exon 4. (*A*) In affected individuals of family F524, a heterozygous C779A substitution was detected resulting in a Thr225Lys amino acid exchange. (*B*) Affected individuals in family F739 showed a heterozygous C849G substitution, causing a Cys248Trp change. (*C*) Affected subjects in F762 carried heterozygously a 12 bp deletion together with an insertion of nine nucleotides (383del12/ins9). The deleted nucleotides are indicated in underlined and bold. The inserted nucleotides are shown in red. Because of this mutation five amino acids are replaced by four different ones. The pedigree was recently published [20]. Arrows denote individuals in whom DNA was available for haplotype analysis.

Table 1. Synopsis of clinical data, imaging results, renal histology and Uromodulin (*UMOD*) mutation of the patients investigated by our study

Family number	Gender	Age at presentation	Age at ESRD/death	Clinical symptoms	Imaging	Histology (kidney biopsy)	Heterozygous mutation (protein changes)
F524							
II-1	M	27	29	CRI, hyperuricemia	NA	Tubulointerstitial atrophy (50%) and fibrosis with interstitial cell infiltration, microcysts	C779A (Thr225Lys)
II-3	M	18	34	CRI, gout, hyperuricemia	US (reduced parenchyma, small kidney, small cysts)	Thickened basement membrane, sclerosed glomeruli (20%), tubular atrophy	C779A (Thr225Lys)
II-4	M	29	NA	CRI, hyperuricemia	MRI (small right kidney, no cysts)	Tubular atrophy (70%), tubulo-interstitial fibrosis, occasional microcysts, thickened basement membrane	C779A (Thr225Lys)
F739							
I-1	M	39	45	CRI, hyperuricemia	US (small kidneys)	NA	C849G (Cys248Trp)
II-1	M	18	NA	CRI, hyperuricemia	US (small kidneys, reduced parenchyma, 1 cyst)	Interstitial fibrosis, atrophic tubuli, sclerosed glomeruli, thickened basement membrane	C849G (Cys248Trp)
II-2	F	17	NA	CRI, hyperuricemia	NA	NA	C849G (Cys248Trp)
F762							
III-5	F	59	60	CRI, hypertension	NA	Interstitial atrophy, occasional microcysts, thickened basement membrane	383del12/ins9 (ValCysProGluGly93-97AlaAlaSerCys)
III-10	F	36	37	CRI, hypertension	NA	NA	383del12/ins9 (ValCysProGluGly93-97AlaAlaSerCys)
III-11	M	NA	56	CRI, hypertension	US (small kidneys, multiple small cysts bilaterally)	NA	383del12/ins9 (ValCysProGluGly93-97AlaAlaSerCys)
IV-1	F	25	51	CRI, hypertension	NA	NA	383del12/ins9 (ValCysProGluGly93-97AlaAlaSerCys)
IV-2	M	49	52	CRI, hypertension	NA	Tubulointerstitial atrophy and fibrosis, occasional microcysts, thickened basement membrane	383del12/ins9 (ValCysProGluGly93-97AlaAlaSerCys)
IV-3	M	42		CRI, hypertension	NA	50% of glomeruli sclerosed, bands of tubulointerstitial atrophy, no microcysts, thickened basement membrane	383del12/ins9 (ValCysProGluGly93-97AlaAlaSerCys)

CRI, chronic renal insufficiency; NA, not available; US, ultrasound; MRI, magnetic resonance imaging. Age at presentation and age at end-stage renal disease (ESRD) is given in years.

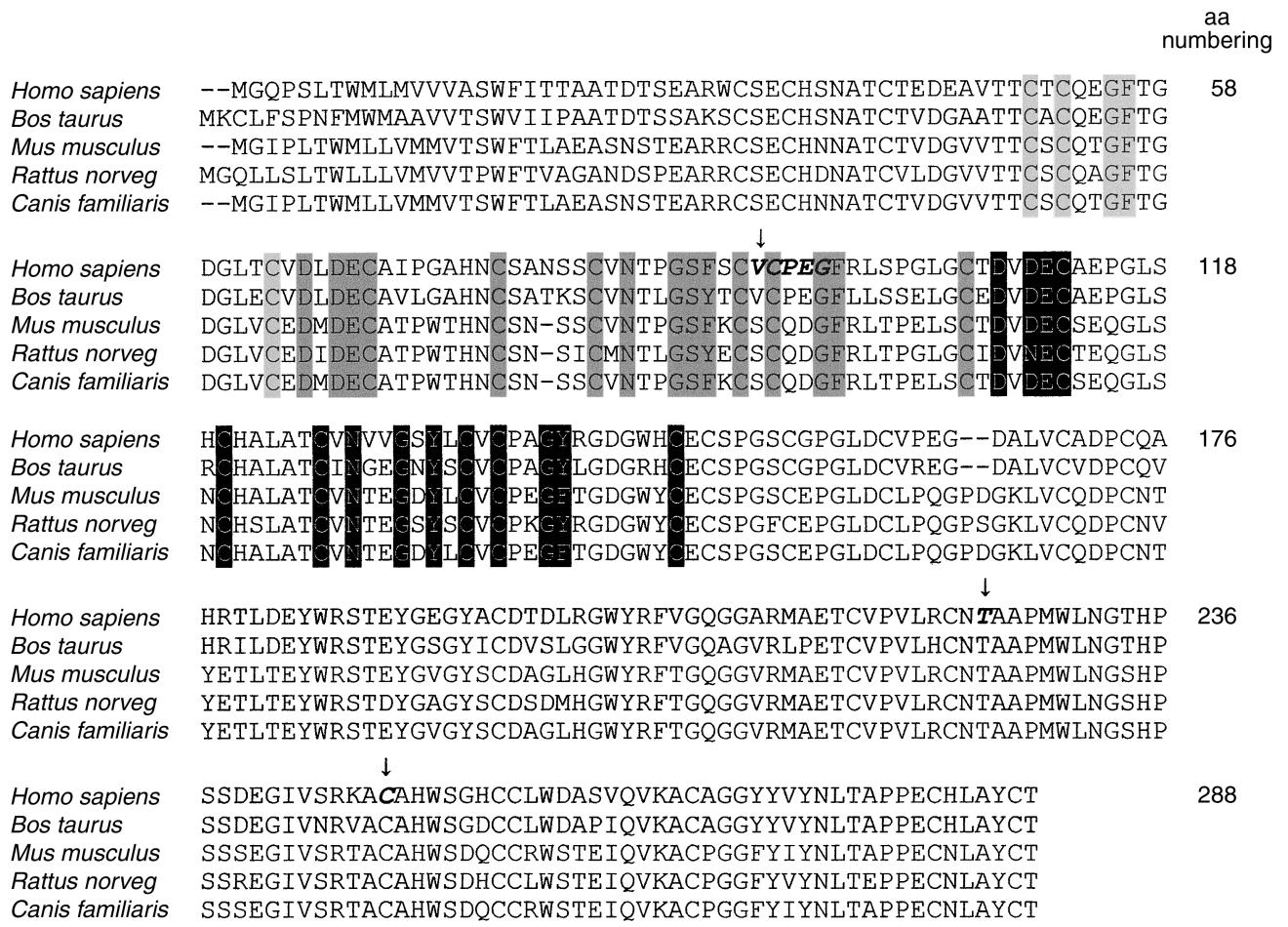

Fig. 2. Comparison of the amino acid conservation in exon 3 and 4 (in which all mutations up to now were found) through evolution, using the CLUSTAL W (1.81) multiple sequence alignment software [27]. Shown is the amino acid sequence of the Uromodulin protein equivalent from *Homo sapiens*, *Bos taurus*, *Mus musculus*, and *Rattus norvegicus*. To underline the high degree of conversation with the zymogen granule membrane protein (*GP2*), the *GP2* amino acid of *Canis familiaris* is indicated in the bottom row. The three calcium-binding endothelial growth facor (EGF)-like domains are highlighted in light gray, dark gray, and black. These domains were found using the consensus sequence of calcium-binding EGF-like domains in the NCBI Conserved Domain Database [28]. The amino acids affected by the mutations identified in patients with MCKD2 are indicated by arrows. Amino acid numbering is shown on the right margin for *Homo sapiens UMOD*.

ciency, hemophilia B, and familial hypercholesterolaemia missense mutations within cbEGF domains were found [22]. Mutations in the *Fibrillin-1* (*FBN1*) cause the Marfan syndrome. *FBN1* reveals an equivalent domain forming a part of a calcium coordinating segment that stabilizes the tertiary structure [23]. Tandem *FBN1* cbEGF domain pairs, when saturated with calcium, exhibit a rod-like conformation [22]. In Marfan syndrome, missense mutations in *FBN1* have been described affecting the same cbEGF domain as the mutation of F762 (383del12/ins9) [24, 25]. Smallridge et al [22] distinguished mutations within cbEGF domains as (*1*) mutations affecting cysteine residues and thereby disrupting disulphide bonds and (*2*) mutations affecting residues in the calcium-binding consensus sequence, which are likely to reduce calcium-binding affinity. As a consequence of the 383del12/ins9 mutation a cysteine is also affected, but the reason for the resulting impaired function remains theoretical because the importance of the four other replaced amino acids (ValProGlyGlu) is unclear.

The Thr225Lys mutation of F524 and the Cys248Trp mutation of F739 are located in a region of unknown function that is also encoded by exon 4. Hart et al [10] and Turner et al [17], repectively, also found two mutations in this region of exon 4, outside the known cbEGF-like domain. Interestingly, this region shows an identity of 56% with *GP2*, another ZP domain-containing protein. All three mutations found are not only conserved in the above-mentioned animals but also in this conserved part of *GP2* of *Canis familiaris*. Two of these mutations (Cys248Trp in F739, 383del12/ins9 in F762) involve cysteine residues, which are highly conserved in the *UMOD* protein throughout evolution including *C. elegans* (Fig. 2). *UMOD* contains 48 cysteine residues per monomer form-

ing 24 intramolecular disulfide bonds. The amino acid changes in F739 and F762 are therefore expected to change the molecular conformation through impaired intra- or intermolecular disulphide bond formation. The high cysteine content of THP and correct formation of the disulphide bonds were suspected to be the rate limiting step for the export of the premature THP out the endoplasmatic reticulum and that this regulates the efficiency of THP maturation [11].

Impaired disulphide binding is well known as a reason for other disorders, for example, diabetes insipidus centralis with a less stable vasopressin precursor, which accumulates in the endoplasmic reticulum [26]. The mutations we found are very likely to cause MCKD2 in these patients, even if none of them is a frameshift or a nonsense mutation. Also Hart et al [10] and Turner et al [17] did not detect any frameshift or nonsense mutation, which would cause a truncated protein. In addition, and surprisingly, all up to now identified mutations with the exception of one mutation at the beginning of the neighboring exon 5 are located in exon 4. All mutations take place in front of the ZP domain. The N-terminal half of exon 4 encodes the three known calcium-binding EGF-like domains [16]. The C-terminal part of exon 4 includes a nine amino acid long immunoglobulin light chain–binding domain [14], which has not been affected by any mutation up to now. However, it seems that exon 4 plays an important role in the function of *UMOD* and that heterozygous mutations in this exon lead to the specific phenotype of MCKD2.

The clinical presentation of the phenotype has to be evaluated very carefully since renal cysts in imaging (only three of 12 affected individuals) and hyperuricemia (six of 12 affected individuals) do not occur in all of the patients. In all affected individuals, renal insufficiency (creatinine clearance <60 mL/min/1.73 m^2) was diagnosed. The age of onset is varied between 17 and 59 years of age. Hart et al [10] also described a kindred, in which the vast majority but not all affected individuals have hyperuricemia. This underlines the heterogeneity of the phenotype and might show that neither hyperuricemia nor cysts are an obligatory feature of the clinical presentation. At the moment, a significant genotype/phenotype correlation is not possible due to the limited number of different mutations detected so far.

Finally, it was surprising to us to find only three mutations in 19 families, which were compatible with linkage to 16p12. This may be explained by the small number of affected persons in most families, possibly resulting in false positive linkage result in an autosomal-dominant disease. Alternatively, a second gene for FJHN and MCKD2 might exist in the more centromeric region of *UMOD* in the region described by Kamatani et al [7] and which excludes the *UMOD* gene. Reports about additional mutations in MCKD2 and studies concerning the function of the *UMOD* protein will help to clarify the role of exon 4 for the pathogenesis of MCKD.

ACKNOWLEDGMENTS

We thank all members of the MCKD families for their participation, R.H. Lyons for excellent large-scale sequencing, and N. Hateboer for contribution of patient material. The outstanding technical assistance of Anita Imm is gratefully acknowledged. Dr. Fuchshuber was supported by a grant from the German Research Foundation (DFG Fu 202/2-1) and the Fritz-Thyssen-Stiftung (1999-2061).

Reprints requests to Friedhelm Hildebrandt, M.D., Department of Pediatrics and Communicable Diseases, University of Michigan, 8220C MSRB III, 1150 West Medical Center Drive, Ann Arbor, MI 48109-0646. E-mail: fhilde@umich.edu

REFERENCES

1. Scolari F, Puzzer D, Amoroso A, *et al*: Identification of a new locus for medullary cystic disease, on chromosome 16p12. *Am J Hum Genet* 64:1655–1660, 1999
2. Waldherr R, Lennert T, Weber HP, *et al*: The nephronophthisis complex: A clinicopathologic study in children. *Virchows Arch* 394:235–254, 1982
3. Hildebrandt F, Otto E: Molecular genetics of nephronophthisis and medullary cystic kidney disease. *J Am Soc Nephrol* 11:1753–1761, 2000
4. Christodoulou K, Tsingis M, Stavrou C, *et al*: Chromosome 1 localization of a gene for autosomal dominant medullary cystic kidney disease. *Hum Mol Genet* 7:905–911, 1998
5. Dahan K, Fuchshuber A, Adamis S, *et al*: Familal juvenile hyperuremic nephropathy and autosomal dominant medullary cystic kidney disease type 2: Two facets of the same disease? *J Am Soc Nephrol* 12:2348–2357, 2001
6. Stiburkova B, Majewski J, Sebesta I, *et al*: Familial juvenile hyperuricemic nephropathy: Localization of the gene on chromosome 16p11.2-and evidence for genetic heterogeneity. *Am J Hum Genet* 66:1989–1994, 2000
7. Kamatani N, Moritani M, Yamanaka H, *et al*: Localization of a gene for familial juvenile hyperuricemic nephropathy causing underexcretion-type gout to 16p12 by genome-wide linkage analysis of a large family. *Arthritis Rheum* 43:925–929, 2000
8. Stiburková B, Majewski J, Hodanová K, *et al*: Familial juvenile hyperuricaemic nephropathy (FJHN): Linkage analysis in 15 families, physical and transcriptional characterisation of the FJHN critical region on chromosome 16p11.2 and the analysis of seven candidate genes. *Eur J Hum Genet* 11:145–154, 2002
9. Pirulli D, Puzzer D, De Fusco M, *et al*: Molecular analysis of uromodulin and SAH genes, positional candidates for autosomal dominant medullary cystic kidney disease linked to 16p12. *J Nephrol* 14:392–396, 2001
10. Hart TC, Gorry MC, Hart PS, *et al*: Mutations of the UMOD gene are responsible for medullary cystic kidney disease 2 and familial juvenile hyperuricaemic nephropathy. *J Med Genet* 39:882–892, 2002
11. Malagolini N, Cavallone D, Serafini-Cessi F: Intracellular transport, cell-surface exposure and release of recombinant Tamm-Horsfall glycoprotein. *Kidney Int* 52:1340–1350, 1997
12. Leeker A, Kreft B, Sandmann J, *et al*: Tamm-Horsfall protein inhibits binding of S- and P-fimbriated *Escherichia coli* to human renal tubular epithelial cells. *Exp Nephrol* 5:38–46, 1997
13. Rhodes DCJ: Binding of Tamm-Horsfall protein to complement 1q and complement 1, including influence of hydrogen-ion concentration. *Immunol Cell Biol* 78:558–566, 2002
14. Ying WZ, Sanders PW: Mapping the binding domain of immunoglobulin light chains for Tamm-Horsfall protein. *Am J Pathol* 158: 18859–18866, 2001
15. Marengo SR, Chen DH, Kaung HL, *et al*: Decreased renal expression of the putative calcium oxalate inhibitor Tamm-Horsfall protein in the ethylene glycol rat model of calcium oxalate urolithiasis. *J Urol* 167:22192–22197, 2002

16. Jovine L, Qi H, Williams Z, *et al*: The ZP domain is a conserved module for polymerization of extracellular proteins. *Nat Cell Biol* 4:457–461, 2002
17. Turner JJO, Stacey JM, Harding B, *et al*: Uromodulin mutations cause familial juvenile hyperuricemic nephropathy. *J Clin Endocrinol Metab* 88:464–470, 2003
18. Wilcox WD: Abnormal serum uric acid levels in children. *J Pediatr* 128:731–741, 1996
19. Available at *http://genome.ucsc.edu/*, accessed on December 15, 2002
20. Hateboer N, Gumbs C, Teare D, *et al*: Confirmation of a gene locus for medullary cystic kidney disease (*MCKD2*) on chromosome 16p12. *Kidney Int* 60:1233–1239, 2001
21. Resnick JS, Sisson S, Vernier RL: Tamm-Horsfall protein: abnormal localization in renal disease. *Lab Invest* 38:550–555, 1978
22. Smallridge RS, Whiteman P, Werner JM, *et al*: Solution structure and dynamics of a calcium binding epidermal growth factor-like domain pair from the neonatal region of human fibrillin-1. *J Biol Chem* 278:12199–12206, 2003
23. Yuan X, Werner JM, Lack J, *et al*: Effects of the N2144S mutation on backbone dynamics of a TB-cbEGF domain pair from human fibrillin-1. *J Mol Biol* 316:113–125, 2002
24. Collod-Beroud G, Beroud C, Ades L, *et al*: Marfan database (third edition): New mutations and new routines for the software. *Nucleic Acids Res* 26:229–233, 1998
25. Rommel K, Karck M, Haverich A, *et al*: Mutation screening of the fibrillin-1 (FBN1) gene in 76 unrelated patients with Marfan syndrome or Marfanoid features leads to the identification of 11 novel and three previously reported mutations. *Hum Mutat* 20:406–407, 2002
26. Fluck CE, Deladoey J, Nayak S, *et al*: Autosomal dominant neurohypophyseal diabetes insipidus in a Swiss family, caused by a novel mutation (C59Delta/A60W) in the neurophysin moiety of prepro-vasopressin-neurophysin II (AVP-NP II). *Eur J Endocrinol* 145:439–444, 2001
27. Available at *http://zeon.well.ox.ac.uk* accessed on February 15, 2003
28. Available at *http://www.ncbi.nlm.nih.gov* accessed on February 16, 2003